JOC The Journal of Organic Chemistry

pubs.acs.org/joc Article

Cooperative Multipoint Recognition of Sialic Acid by Benzoboroxole-Based Receptors Bearing Cationic Hydrogen-Bond Donors

Alice Di Pasquale, Stefano Tommasone, Lili Xu, Jing Ma, and Paula M. Mendes*

Cite This: J. Org. Chem. 2020, 85, 8330−8338 Read Online

ACCESS | Metrics & More | Article Recommendations | Supporting Information

ABSTRACT: Sialic acid recognition remains an interesting and challenging target in molecular receptor design. Herein, we report a series of benzoboroxole-based receptors in which cationic hydrogen-bond donors have been introduced and shown to promote multipoint sialic acid recognition. One striking feature revealed by these receptors is that the carboxylate sialic acid residue is the primary binding determinant for recognition by benzoboroxole, in which the presence of charge-reinforced hydrogen bonds results in enhanced selectivity for sialic acid over other carbohydrates and a 4.5-fold increase in affinity. These findings open up wide possibilities for benzoboroxole-based receptors use in life science research, biotechnology, and diagnostics.

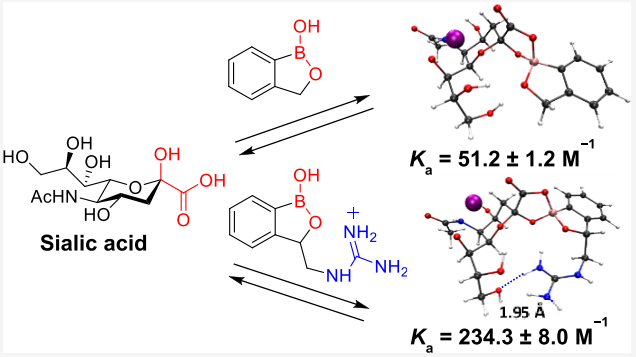

INTRODUCTION

Sialic acid (SA) is a ubiquitous negatively charged monosaccharide that partakes in many important biological roles.[1,2] SA exists in two different configurations; when free in solution, it is present predominately in the β anomeric configuration (>95%), while the α anomer occurs when bound to other sugar residues.[3] SA can be found at the terminal end of glycans that decorate cell surfaces and mediate biological processes such as cell signaling, growth, and differentiation.[1] Changes in SA levels or expression can indicate undergoing pathological conditions. Moreover, alteration of its lysosomal storage causes rare neurodegenerative conditions that are referred to as sialic acid storage diseases, characterized by high levels of sialic acid in urine.[4] Alternatively, increased expression of sialic acid at the terminal end of glycoproteins occurs in cancer cells as a defense mechanism from the immune system.[5,6] Due to the many biological functions in which sialic acid is involved, its recognition plays an important role in life science research, diagnostics, and therapeutics.

Phenylboronic acids have been extensively employed as receptors to detect carbohydrates, including sialic acid.[7−11] The analogues benzoboroxoles,[12] cyclic phenylboronic acid esters, have a higher affinity for monosaccharides.[8,13,14] Nevertheless, there are not many examples of benzoboroxole-based receptors for the detection of sialic acid. The binding affinity of boron-based receptors for sialic acid is reported to be enhanced at acidic pH,[15] unlike other monosaccharides that are bound at basic pH.[16] Most of the boron-based receptors that target sialic acid have been developed considering the *cis*-diol, either C7/C9 or C8/C9, of the glycerol chain being the binding site. The receptors, in addition to the boronic acid unit, often present other functional groups, such as amino groups,[10] heterocyclic rings,[17] and urea moieties,[18] which are reported to interact with the carboxylate group.

Alternatively, other theories regarding the binding site have been postulated. Djanashvili et al. proposed a model in which the binding site is pH-dependent.[19] The glycerol chain is considered the main binding site at pH > 8, while at pH 2−8 the binding occurs via the α-hydroxyacid group, thus through the carboxylate and the vicinal hydroxyl group. Moreover, Nishitani et al. have proposed that the binding of boronic acid receptors occurs exclusively with the α-hydroxyacid (Figure 1).[20]

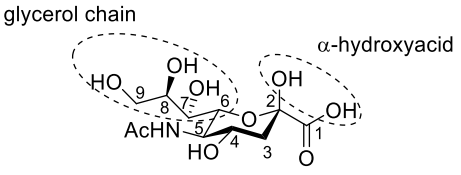

Figure 1. Two possible binding sites of sialic acid.

Received: February 18, 2020
Published: June 8, 2020

Herein, the interaction between nonfunctionalized benzoboroxole and sialic acid was studied, leading to the unequivocal identification of the binding site. Consequently, a series of positively charged benzoboroxole receptors were designed and synthesized to promote further interactions and stronger binding with sialic acid. The binding affinity between the different receptors and sialic acid was determined using isothermal titration calorimetry (ITC), allowing us to uncover important cooperative binding effects. The molecular interactions responsible for this synergetic behavior are discussed on the basis of density functional theory calculations.

RESULTS AND DISCUSSION

Binding Site. The binding affinity of the nonfunctionalized benzoboroxole receptor **1** to sialic acid (**2**) and 2-*O*-methyl-α-sialic acid (**3**) (Figure 2) was measured by ITC at three

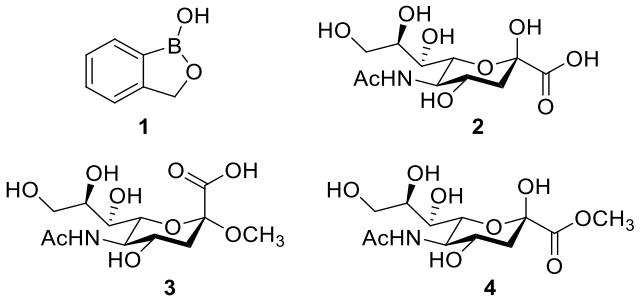

Figure 2. Nonfunctionalized benzoboroxole receptor (**1**), β-sialic acid (**2**), 2-*O*-methyl-α-sialic acid (**3**), and β-sialic acid methyl ester (**4**).

different pH values (5.5, 7.4, and 10.0). 2-*O*-Methyl-α-sialic acid **3** was used as a model molecule for the α configuration resembling sialic acid in glycoproteins (Figure 2).

In sialic acid (**2**), both the glycerol chain and the α-hydroxyacid binding sites are available, while in **3** the methoxy group in position 2 prohibits binding with the α-hydroxyacid. For the aforementioned ligands, the glycerol chain is always available for binding. Consequently, if binding occurs predominantly via the glycerol chain,[17] both sugars **2** and **3** should bind to receptor **1** across the studied pH range.

Another model predicts that the binding site is pH-dependent, where binding occurs with the α-hydroxyacid below pH 8 and with the glycerol chain under more basic conditions.[19] Under the assumption that this model holds, **1** would bind **2** under all conditions, while the interaction with **3** would only occur at pH > 8. The data in Table 1 indicates that there is no significant binding between **1** and **3**; therefore, the availability of α-hydroxyacid is pivotal for the binding to occur. The lack of binding to α-sialic acid is also reported in the literature with binding constants K_a < 10 M^{-1}.[21,22] To support this hypothesis, the binding of receptor **1** to sialic acid methyl ester **4** (Figure 2) was measured at pH 5.5, with no significant binding detected by ITC, thus confirming the participation of α-hydroxyacid in the binding events.

To confirm these findings, 1:1 mixtures of **1** with **2** and **3**, respectively, were investigated by NMR and mass spectrometry (MS) analyses. The ^{1}H NMR spectrum of receptor **1** showed four protons of the aromatic ring as three multiplets in the 7.70−7.25 ppm region (Figure 3a).

The ^{1}H NMR spectrum of the **1**−**2** mixture presented the aromatic region signals of unbound receptor **1**, which were shifted by ∼0.05 ppm due to changes in the environment, and

Table 1. ITC-Binding Studies of Receptor 1 with Sialic Acid (2), 2-*O*-Methyl-α-sialic Acid (3) and Sialic Acid Methyl Ester (4) at pH 5.5 (0.1 M Acetate Buffer), 7.4 (0.1 M Phosphate Buffer), and 10.0 (0.1 M Ammonium Acetate Buffer) at 25 °C[a]

	K_a (M^{-1})		
pH	**2**	**3**	**4**[b]
5.5	51.2 ± 1.2	1.6 ± 2.4	<1.0
7.4	39.3 ± 0.6	<1.0	
10.0	12.5 ± 2.5	<1.0	

[a]Each experiment consists of three titrations. The heat of dilution was measured and subtracted. [b]The binding affinity of **1** to sialic acid methyl ester **4** was not measured at pH ≥ 7.4 due to the fast hydrolysis of the ester group.

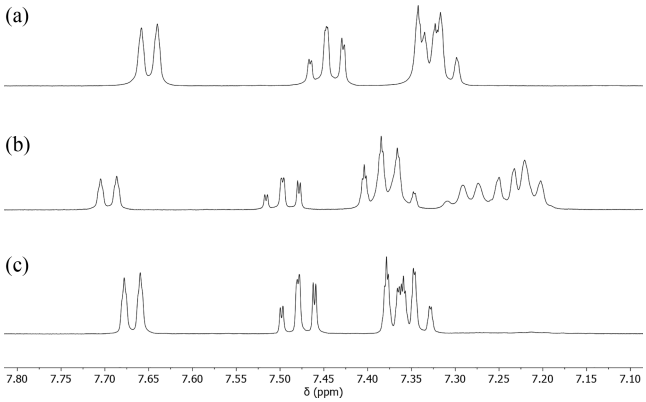

Figure 3. ^{1}H NMR spectra in 0.1 M CD_3COOD at 400 MHz and 298 K: (a) **1**; (b) 1:1 mixture **1**−**2**; and (c) 1:1 mixture **1**−**3**.

additional peaks between 7.32 and 7.19 ppm (Figure 3b), which are could be ascribed to the complexed species as their intensity changed upon different receptor/ligand ratios (Figure S22). On the other hand, the analysis of the **1**−**3** mixture showed only three sets of multiplets corresponding to the unbound **1** shifted by ∼0.02 ppm, confirming that there is no complexation with α-sialic acid (Figure 3c). The presence of the complexed species in the **1**−**2** mixture was also confirmed by electrospray ionization ESI (−) MS analysis, where a peak at m/z = 424.14 $[M]^-$ was observed (Figure S41), while a similar analysis of the **1**−**3** mixture showed only the peaks of unbound species (Figure S42).

Furthermore, the binding affinity of **1** for **2** is pH-dependent. At pH 5.5, the measured binding constant is K_a= 51.2 ± 1.2 M^{-1}, which decreases at more basic pH values, with K_a= 12.5 ± 2.5 M^{-1} at pH 10 (Table 1). This pH-dependent binding profile has been previously seen for the binding of boronic acids to other α-hydroxyacids, such as lactic[23] and tartaric acid.[24] The complexation between boronic acid derivatives and an α-hydroxyacid has been reported as occurring predominantly at acidic pH (pH < pK_a); therefore, the complexation occurs between sialic acid and trigonal benzoboroxole (Figure 4). On the other hand, at pH ≥ 7.4 (pK_a of **1** is 7.2)[8] there is electrostatic repulsion between the boronate ion and the carboxylate ion that needs to be overcome for the complexation to occur, hence the lower binding affinity at pH ≥ 7.4.

The results of the above-described experiments allow us to conclude that the α-hydroxyacid is the site through which boron-based receptors bind sialic acid rather than the glycerol chain, as previously reported. This is a very important finding

https://dx.doi.org/10.1021/acs.joc.0c00173
J. Org. Chem. 2020, 85, 8330−8338

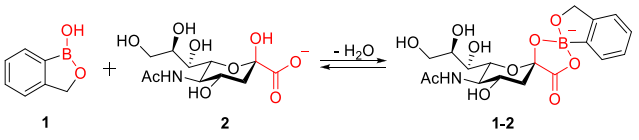

Figure 4. Equilibrium between receptor **1** and sialic acid **2** to give the boronate ester complex at acidic pH.

since it provides the rationale for developing benzoboroxole-based receptors with enhanced binding affinity and selectivity for sialic acid. With this provision in mind, we have designed and synthesized a series of positively charged benzoboroxoles.

Design and Synthesis of Benzoboroxole Receptors. Synthetic receptors that interact with sialic acid solely through noncovalent interactions have been developed and consist of an aromatic core and positively charged branches.[25,26] Herein, we combine covalent and noncovalent interactions by designing receptors **5**−**10** (Figure 5) with a benzoboroxole unit bearing an amino or a guanidino group. In addition, derivatives **9** and **10** are functionalized with an aromatic side chain that can provide CH−π interactions, as seen in lectins.[27,28]

Receptor **5** was synthesized from 2-formylphenylboronic acid to give initially the nitrofunctionalized benzoboroxole, which was then reduced with $NiCl_2$ and $NaBH_4$ to give the Boc-protected amine derivative.[29] The protection was cleaved with 2 M HCl in Et_2O. Receptors **7** and **9** were synthesized via the coupling of **5** with Boc-glycine-OH and 4-(Boc-aminomethyl)benzoic acid, respectively, in the presence of 1-ethyl-3-(3-dimethylaminopropyl)carbodiimide (EDCI) and 4-dimethylaminopyridine (DMAP) (Scheme 1).

Guanidino derivatives **6**, **8**, and **10** were synthesized from the corresponding amino derivatives **5**, **7**, and **9**, respectively, with *N*,*N*′-di-Boc-1*H*-pyrazole-1-carboxamidine to give the Boc-protected derivative. The deprotection was initially attempted with 2 M HCl in Et_2O and trifluoroacetic acid (TFA) in methanol, affording only a partial cleavage of the Boc groups. The complete cleavage of the Boc groups was achieved by generating hydrochloric acid in situ adding acetyl chloride to a mixture of methanol and ethyl acetate at 0 °C.

Given the chirality of the synthesized receptors **5**−**10**, these were used as racemic mixtures for all of the studies presented herein.

ITC-Binding Studies. The binding affinities of receptors **5**−**10** to sialic acid were evaluated by ITC at pH values of 5.5, 7.4, and 8.5 (Figure 6), with a binding model postulated. All synthesized receptors, **5**−**10**, present an increase in the binding affinity when compared to nonfunctionalized receptor **1**. This can be ascribed to the presence of the positively charged group that creates charge-reinforced hydrogen bonds[25] with sialic acid H-bond acceptors, resulting in stabilization of the boronate ester. All synthesized receptors, **5**−**10**, achieved their highest affinity toward sialic acid at pH 5.5 with an increase of 2- to 4.5-fold in the binding constants, when compared to nonfunctionalized benzoboroxole **1**.

The enhanced binding affinity occurring at acidic pH is due to the lack of repulsion between the receptors and the binding site, as seen for **1**, and to the contribution of the charge-reinforced hydrogen bonds. Differences in the affinities are also attributed to the different buffer solutions (sodium acetate, phosphate, and ammonium acetate buffer) used for the studies at the selected pH values.[30] Furthermore, the guanidino moiety has a greater effect in enhancing the binding affinity when compared to the amino group. This effect can be seen especially for receptors **5** and **6**. At pH 5.5, receptor **5** presents a binding constant of 150.4 ± 7.9 M^{-1}, while the corresponding guanidino derivative, **6**, has a 1.5 times greater binding constant (K_a = 234.3 ± 8.0 M^{-1}). The guanidino moiety provides additional charge-reinforced hydrogen bonds, creating a wider network of interactions that results in further stabilization of the complex, hence the higher binding affinity.

An enhancement in the affinity, although reduced when compared to the aforementioned receptors, was also observed for receptors **7** (K_a = 129.6 ± 0.8 M^{-1}) and the corresponding guanidino derivative **5** (K_a = 141.0 ± 8.0 M^{-1}). On the other hand, **9** (K_a = 104.4 ± 5.2 M^{-1}) and **10** (K_a = 110.2 ± 3.4 M^{-1}) present a similar binding constant, within error, suggesting that the positively charged moiety does not participate in the binding. Therefore, the side chain plays a role in the complexation, with the affinity being reduced when it is either rigid or longer, as seen for derivatives **7**−**10**. These findings indicate that, for receptors **9** and **10**, the rigid aromatic structure might be blocking the amino and guanidino groups in unsuitable conformations, preventing the formation of charge-reinforced hydrogen bonds between the positively charged moiety and sialic acid. The enhanced binding of receptors **9** and **10**, when compared to **1**, suggests the presence of another type of noncovalent interaction with the ligand, such as CH−π interactions. CH−π interactions are often seen in sialic acid-specific lectins[27,28] and occur between the aromatic moiety and the sialic acid backbone. The contribution to the binding of these interactions is reduced in comparison to charge-reinforced hydrogen bonds, hence the lower binding affinities of **9** and **10** versus the other synthesized receptors at pH 5.5.

Conversely, at basic pH, the affinity toward sialic acid decreases, suggesting that the charge-reinforced hydrogen

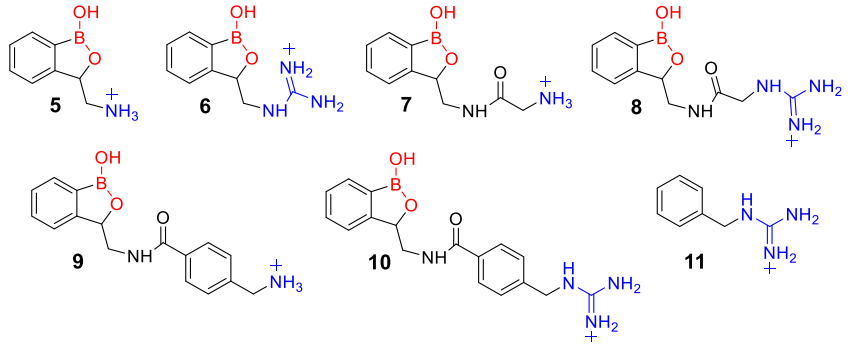

Figure 5. Benzoboroxoles receptors **5**−**10** and control molecule **11**.

https://dx.doi.org/10.1021/acs.joc.0c00173
J. Org. Chem. 2020, 85, 8330−8338

Scheme 1. Synthesis of Benzoboroxole Receptors[a]

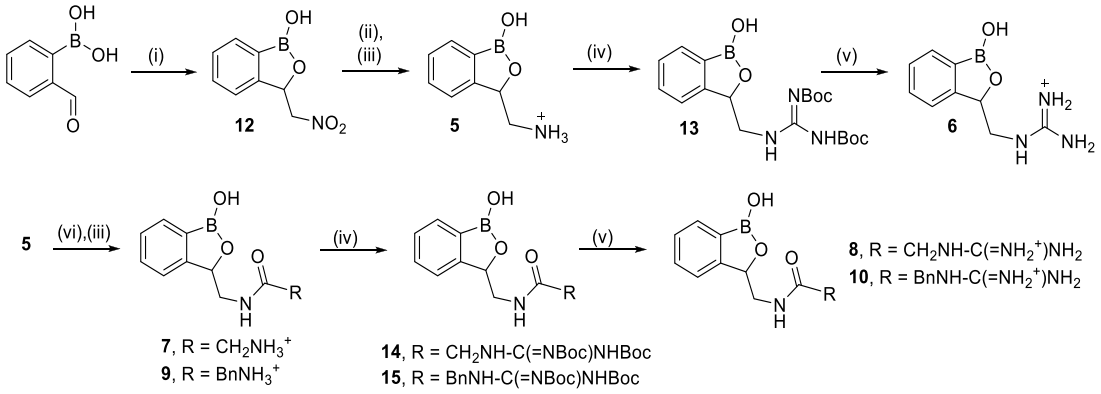

[a](i) CH_3NO_2, NaOH, H_2O; (ii) Boc_2O, $NaBH_4$, $NiCl_2{\cdot}6H_2O$, MeOH; (iii) 2 M HCl in Et_2O; vi *N*,*N*′-di-Boc-1*H*-pyrazole-1-carboxamidine, Et_3N, MeOH; (v) AcCl, MeOH, EtOAc; (vi) Boc-Gly-OH or 4-(Boc-aminomethyl)benzoic acid, DMAP, EDCI, dimethylformamide (DMF).

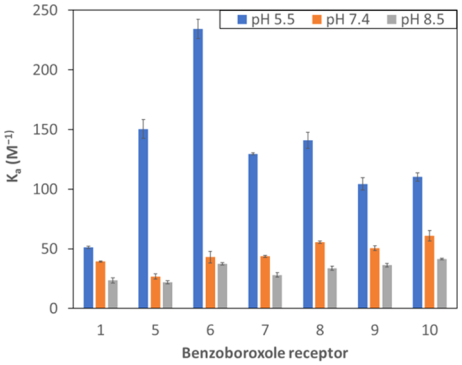

Figure 6. Isothermal titration calorimetry binding studies of receptors **1** and **5**−**10** with sialic acid (**2**) at pH 5.5 (0.1 M acetate buffer), 7.4 (0.1 M phosphate buffer), and 8.5 (0.1 M ammonium acetate buffer) and 25 °C. Each experiment consists of three titrations. The heat of dilution was measured and subtracted.

bonds have a reduced effect on the complexation at this pH. All receptors, but receptor **5**, present at basic pH higher affinity than nonfunctionalized benzoboroxole **1**, suggesting the presence of other noncovalent interactions (e.g., neutral hydrogen bonds, CH−π interactions). For instance, receptor **10**, functionalized with an aromatic side chain, has the highest binding affinity to **2** at pH 8.5, yielding K_a = 41.4 ± 0.6 M^{-1}.

All binding studies were conducted with the racemic mixture of the positively charged receptors; hence, the binding constants of the enantiomeric pure benzoboroxoles were not assessed directly. The shape of the ITC curve indicates whether two enantiomers have similar binding constants or whether one presents a higher affinity.[31] If the binding constant of the two enantiomers, for a given receptor, was significantly different, the titration curves would be composed of two curves and therefore would present a step. Herein, the ITC curves for receptors **5**−**10** (for ITC graphs, see the Supporting Information (SI)) are composed of only one curve and do not present a step. Thus, it is reasonable to assume that both enantiomers, for a given receptor, have similar binding constants for sialic acid and that these do not differ greatly from the binding constant of the racemic mixture.

Furthermore, the cooperative nature of the binding was investigated. A control molecule (**11**) functionalized with a guanidino group, but without the benzoboroxole unit, was synthesized, and its affinity to sialic acid was measured at pH 5.5. Under these conditions, the guanidino moiety can form hydrogen bonds or electrostatic interactions with **2**; however, these interactions are negligible, as no significant binding is detected by ITC.

Therefore, in the binding mechanism, the benzoboroxole unit binds covalently to sialic acid α-hydroxyacid with the formation of a boronate ester, which was proven to be essential for the binding to occur. Subsequently, the reversible complex is stabilized by noncovalent interactions, in particular charge-reinforced hydrogen bonds, resulting in an increase in the binding affinity. Charge-reinforced hydrogen bonds occur between the cationic group (amino or guanidino), and H-bond acceptors of sialic acid,[25] such as the hydroxyl groups. No hydrogen bonds are formed with the carboxylate as this is engaged in an ester with the benzoboroxole unit. Similar behavior is shown in other boron-based receptors containing a guanindino unit,[32] where the preferred interaction of the ligand α-hydroxyacid group is with the boronic acid rather than the guanidino unit. In addition to H-bonds, CH−π interactions stabilize the complex with sialic acid, although these interactions are weaker and thus their effect on the binding is reduced.

Enthalpy−Entropy Compensation (EEC). The ITC experiments, in addition to K_a, provide information about the change in enthalpy (ΔH, kcal mol^{-1}) and entropy (ΔS, cal mol^{-1} deg^{-1}) of the system (for experimental values, see the SI). The experiments were conducted at 25 °C (298.15 K). The change in enthalpy is negative, as the binding event causes the release of heat. On the other hand, the entropy component is negative and unfavorable to the binding due to the loss of degrees of freedom of the two species when bound together.

When plotting the enthalpic component (ΔH) against the entropic one ($T\Delta S$), a linear dependency can be found, indicating an enthalpy−entropy compensation (EEC) effect. In Figure 7, the slopes of the linear dependency are 0.80, 1.02, and 0.86 for pH values of 5.5, 7.4, and 8.5, respectively. When the slope is 1, the EEC is complete. Slopes below <1 indicate that the binding is more sensitive to changes in the entropy of the system, while slopes >1 indicate that the binding in more sensitive to the enthalpic component.[33] The EEC effect is a characteristic of all weak intramolecular interactions in aqueous (aq) systems[34] and thus also to the boronate ester formation between benzoboroxole and sialic acid. The EEC effect was previously shown for other positively charged boronic acid receptors.[32]

https://dx.doi.org/10.1021/acs.joc.0c00173
J. Org. Chem. 2020, 85, 8330−8338

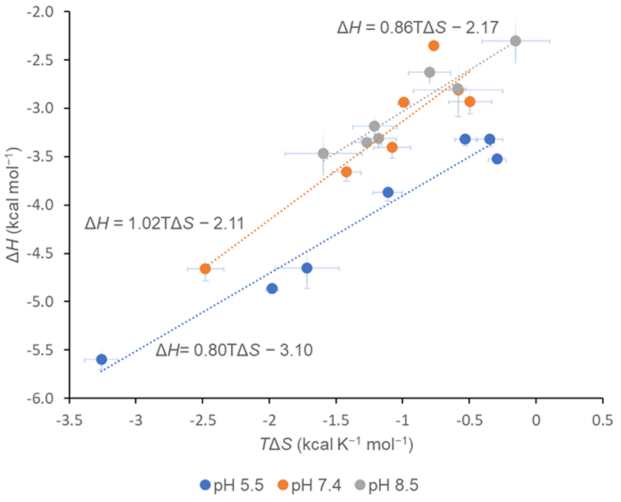

Figure 7. Enthalpy (ΔH) against entropy ($T\Delta S$) plot at pH 5.5 (0.1 M acetate buffer), 7.4 (0.1 M phosphate buffer), and 8.5 (0.1 M ammonium acetate buffer) and 25 °C (298.15 K).

Theoretical Study of the Binding Affinity. The multipoint cooperative binding model was supported by both molecular dynamics (MD) simulations and density functional theory (DFT). The geometries of the complex of the benzoboroxole derivatives **1** and **5**−**10** with sialic acid **2** were optimized using DFT as implemented in the Gaussian program[35] at the level of M06-2X/6-31+G(d,p). The binding energies of nonfunctionalized benzoboroxole receptor **1** and functionalized receptors **5**−**10** with sialic acid were then calculated at the same theoretical level, with the results shown in Figure 8 and Table S5.

The binding energy (E_b) is defined in eq 1

$$E_b = E_{complex} - (E_{SA} + E_{receptor}) \quad (1)$$

where $E_{complex}$, E_{SA}, and $E_{receptor}$ are the total energy of complex and the individual energies of **2** and the benzoboroxole receptor, respectively. The more negative the value of the binding energy (E_b), the stronger the interaction between the benzoboroxole derivatives and sialic acid. Simple computational models were used to differentiate between strong and weak binders according to DFT binding energies (Figure 8). A trend was identified in the strength of interaction with the target being **5**−**8** > **9**−**10** ≫ **1**, which is in agreement with the ITC data. All computational studies presented herein are performed with the *S* enantiomers of the receptors. In addition, for benzoboroxoles **5** and **9**, the binding energies for the *R* enantiomers were calculated and found to be of similar magnitude to the binding energies of the *S* enantiomers. This indicates that both enantiomers have a comparable affinity to sialic acid, as suggested by ITC. Furthermore, the results in Figure 8 were compared to the results obtained from different DFT functionals, M06-2X versus B3LYP, which confirmed the same trend in binding energies. The strong binding for receptors **5**−**8** is ascribed to N−H···O charge-reinforced hydrogen-bonding interactions (with the H···O bond length given in Figure 8) with the glycerol chain. When hydrogen bonds are not present, the interaction with the target is significantly weaker. For instance, receptors **9** and **10** do not form hydrogen bonds with sialic acid but instead provide weaker noncovalent interactions (e.g., CH−π interactions), resulting in medium strength complexation with the target. Receptor **1** does not provide any additional noncovalent interactions, hence the weak binding. For complexes **1**−**2** and **5**−**2**, the binding was also assessed using more complex computational models, such as the implicit solvation model based on density (SMD), shown in Figure S43, and explicit solvent model (Figures S44 and S45). These models agree with the gas-phase model in concluding that the binding occurs with the α-hydroxyacid moiety. Therefore, the binding

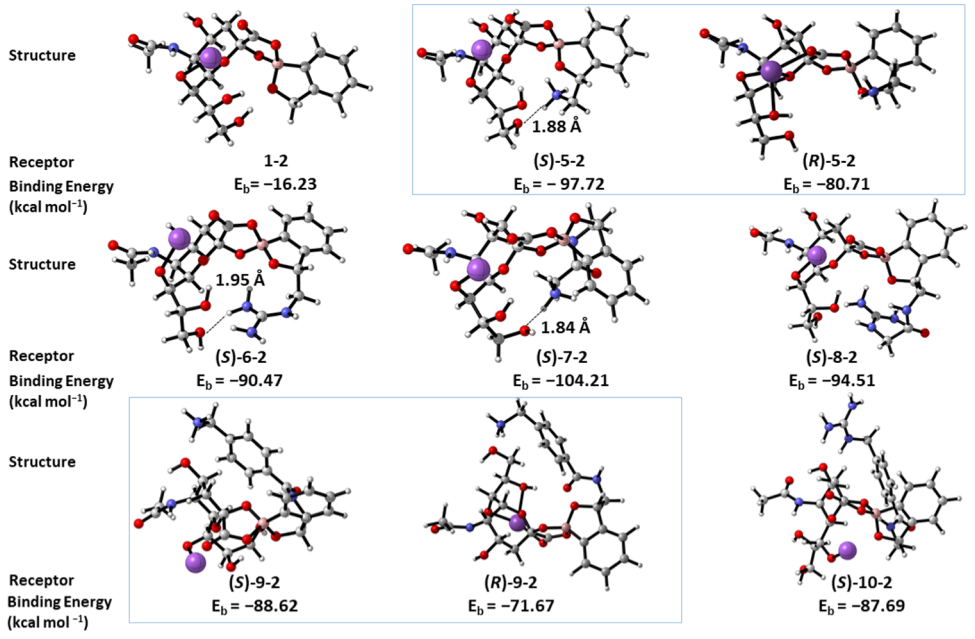

Figure 8. Binding energies (E_b, in units of kcal mol^{-1}) and corresponding structures of interaction between sialic acid **2** and receptor **1**; the *S* enantiomers of receptors **1**, **6**−**8**, and **10**; and the *R* and *S* enantiomers of receptors **5** and **9**. The DFT calculations were carried out at the level of M06-2X/6-31+G(d,p). The N−H···O hydrogen bonds were displayed by the dotted line. The purple ball indicates the counterion (Na^+) in computation models.

https://dx.doi.org/10.1021/acs.joc.0c00173
J. Org. Chem. 2020, 85, 8330−8338

energies of all receptors **1** and **5**−**10** predicted by the gas-phase model are reasonable.

Selectivity Studies. In addition to the binding affinities to sialic acid, the selectivity of receptors **1**, **5**, and **6** to other monosaccharides (e.g., fructose, galactose, glucose, mannose, and glucuronic acid) was assessed at pH 5.5 by ITC. Nonfunctionalized receptor **1** is shown, in Table 2, to be selective for sialic acid under acidic conditions as the affinity to other monosaccharides is greatly reduced for pH values below the pK_a of **1**.[8] Conversely, functionalized receptors **5** and **6** have an increased affinity toward monosaccharides when compared to **1**, as they form charge-reinforced hydrogen bonds with the ligands.

Table 2. ITC-Binding Constants (K_a, M^{-1}) of Receptors 1, 5, and 6 with Sialic Acid, D-Fructose, D-Galactose, D-Glucose, D-Mannose, and D-Glucuronic Acid at pH 5.5 and 25 °C[a]

	1	5	6
sialic acid	51.2 ± 1.2	150.4 ± 7.3	234.3 ± 8.0
D-fructose	18.5 ± 0.6	198.6 ± 16.1	162.6 ± 12.6
D-galactose	7.5 ± 0.4	10.6 ± 4.1	5.6 ± 2.4
D-glucose	<1.0	10.1 ± 4.4	10.0 ± 0.9
D-mannose	<1.0	9.6 ± 4.2	4.8 ± 1.1
D-glucuronic acid	<1.0	11.6 ± 2.2	12.5 ± 0.3

[a]Each experiment consists of three titrations. The heat of dilution was measured and subtracted.

Furthermore, when considering the interaction of positively charged receptors **5** and **6** to negatively charged glucuronic acid, the binding affinity is consistent with the affinity toward neutral glucose, a neutral glucuronic acid analogue. This confirms that the possible electrostatic interaction between positively charged amino or guanidino group and negatively charged carboxylic acid does not play a role in binding, as seen for sialic acid and control **11**. Therefore, there is no cross-reactivity with anionic species. The charge-reinforced hydrogen bonds are particularly significant for the interaction with fructose, with **5** and **6** yielding a binding constant 11 and 9 times greater, respectively, than the binding affinity of receptor **1**. Therefore, the binding of charged receptors is cooperative toward other monosaccharides, as well as sialic acid. For receptor **5** $K_{a\ \text{fructose}} > K_{a\ \text{sialic acid}}$, indicating that **5** is more selective for fructose. On the other hand, receptor **6** is selective for sialic acid at pH 5.5 with $K_{a\ \text{fructose}} = 162.6 \pm 12.6\ M^{-1}$ and $K_{a\ \text{sialic acid}} = 243.3 \pm 8.0\ M^{-1}$.

CONCLUSIONS

In conclusion, we have identified unequivocally that boron-based receptors bind sialic acid exclusively through the α-hydroxyacid group, leading to the formation of boronate esters. Prompted by this knowledge, we have rationally designed and synthesized a new group of benzoboroxole-based receptors, which contain additional sites for sialic acid interaction. The new receptors **5**−**10** display enhanced affinity for sialic acid, when compared to the nonfunctionalized benzoboroxole receptor **1**. The highest binding affinity for all receptors **5**−**10** is achieved at pH 5.5, where charge-reinforced hydrogen bonds with sialic acid are particularly relevant in stabilizing the complex and there is no electrostatic repulsion between the ligand and receptor. In addition, guanidino-functionalized receptors often present a higher binding affinity than the corresponding amino-functionalized receptors, with the creation of wider networks of hydrogen bonds further stabilizing the complex. The presence of charged-reinforced hydrogen bonds between the positively charged amino or guanidino group and the glycerol chain of sialic acid has been confirmed by DFT studies. In addition, the side chain of the receptor has also been seen to play a significant role in the binding affinity. Receptors **7**−**10**, characterized by longer and more rigid side chains, showed reduced binding when compared to **5** and **6** at acidic pH. Furthermore, the multipoint cooperative nature of the binding has been verified with control molecule **11**, for which the absence of the benzoboroxole unit results in no significant binding occurring with sialic acid. Hence, the formation of the boronate ester is pivotal for any interaction to occur between the receptor and the ligand. The highest binding affinity for sialic acid was found under acidic conditions using the guanidino-functionalized receptor **6**. Further studies have shown selectivity of this receptor for sialic acid among other monosaccharides. This work provides valuable insights into effective molecular interactions for sialic acid recognition and a new synthetic receptor, **6**, with improved affinity and selectivity for such a biologically important carbohydrate.

EXPERIMENTAL SECTION

General Comments. Reagents were purchased from Sigma-Aldrich, Acros Organics, and Alfa Aesar. *N*-Acetylneuraminc acid and 2-*O*-methyl-α-D-*N*-acetylneuraminic acid were purchased from Carbosynth Limited. All of the reagents were used without further purification. ^{1}H NMR and ^{13}C NMR spectra were recorded at room temperature (RT) using the following spectrometers: Bruker AVIII400 at 400 and 101 MHz, respectively, and Bruker Ascend 400 at 400 and 101 MHz, respectively. Thin-layer chromatography (TLC) was performed using commercially available Macherey-Nagel aluminum backed plates coated with a 0.20 mm layer of 60 Å silica gel with a fluorescence indicator UV254. TLC plates were visualized using ultraviolet light of 254 nm wavelength. Silica gel column chromatography was carried out using Sigma-Aldrich 60 Å silica gel (35−70 μm). Mass spectra were recorded with a Bruker Daltonics MicrOTOF-Q II spectrometer.

*General Procedure (**A**) for the Synthesis of Boc-Amine Benzoboroxole Derivatives.* 7-(Aminomethyl)benzoxaborole hydrochloride (**5**) (0.10 g, 0.50 mmol) was dissolved in DMF (5 mL). DMAP (0.15 g 1.25 mmol) was added followed by the addition of either Boc-Gly-OH or 4-(Boc-aminomethyl)benzoic acid (0.11g, 0.60 mmol) and 1-ethyl-3-(3-dimethylaminopropyl)carbodiimide (EDCI) (0.12 g, 0.60 mmol). The reaction mixture was stirred overnight; then, the solvent was evaporated under reduced pressure. The crude was dissolved in ethyl acetate and washed with 1 M HCl (3 × 5 mL) and sat. aq $NaHCO_3$ (5 mL). The organic layer was dried with $MgSO_4$ and concentrated under reduced pressure to give the Boc-amine benzoboroxole derivatives, which were not isolated.

*General Procedure (**B**) for the Synthesis of Amino Benzoboroxole Receptors.* Boc-amine benzoboroxole derivative was stirred overnight with 2 M HCl in Et_2O (10 mL), and the solvent was removed either by filtration or evaporation under vacuum.

*General Procedure (**C**) for Boc-Guanidine Benzoboroxole Derivatives.* Amino-functionalized benzoboroxole derivative (**5**, **7**, and **9**) (0.20 g, 1.00 mmol) was dissolved in methanol (15 mL). *N*,*N*′-di-Boc-1*H*-pyrazole-1-carboxamidine (0.25 g, 1.00 mmol) and triethylamine (324 μL, 2.32 mmol) were added, and the mixture was stirred overnight. The solvent was removed under vacuum, and the crude was purified by column chromatography on silica gel.

*General Procedure (**D**) for Guanidino Benzoboroxole Derivatives.* Boc-guanidine benzoboroxole derivative (**14**, **15**, and **16**) (0.10 g, 0.25 mol) was dissolved in a mixture of EtOAc (5 mL) and MeOH (2 mL). The mixture was cooled to 0 °C, and acetyl chloride (0.5

https://dx.doi.org/10.1021/acs.joc.0c00173
J. Org. Chem. 2020, 85, 8330−8338

mL) was added dropwise. The reaction was stirred at RT for 48−72 h, and the solvent was removed under vacuum.

Synthesis of ***12***. 2-Formylphenylboronic acid (1.92 g, 12.82 mmol) was dissolved in 12.78 mL of water. The solution was cooled to 0 °C, and nitromethane was added (2.076 mL, 38.33 mmol) followed by the addition of NaOH (0.54 g, 13.50 mmol). The reaction mixture was stirred for 3 h, diluted, and acidified with 2 M HCl. The precipitate was filtered to give pure **12** as a white-yellow solid (2.37 g, 92%). ^{1}H NMR spectra are in agreement with the literature.[36]

Synthesis of ***5***.[29] A solution of **12** (0.50 g, 2.59 mmol) in anhydrous methanol was cooled to 0 °C. $(Boc)_2O$ (1.2 mL, 5.22 mmol) and $NiCl_2{\cdot}6H_2O$ (0.62 g, 2.96 mmol) were added, and the mixture was stirred under argon for 20 min. $NaBH_4$ (0.59 g, 15.59 mmol) was added, and the mixture was stirred overnight at RT. The solvent was evaporated under reduced pressure, and the crude was dissolved in EtOAc and filtered through Celite. The solution was concentrated under reduced pressure, and the crude was deprotected overnight with 2 M HCl in Et_2O (15 mL). The precipitated was filtered and triturated with Et_2O to give derivative **5** as an off-white solid (0.40 g, 78%). ^{1}H NMR spectra are in agreement with the literature.[29]

Synthesis of ***7***. Derivative **7** was synthesized from **5** following procedure A. The crude was not purified further and the deprotection was performed following procedure B. The precipitated was filtered and triturated with Et_2O to give derivative **7** as an off-white solid. (40.2 mg, 31%). ^{1}H NMR (400 MHz, dimethyl sulfoxide (DMSO)-d_6, 298 K) δ ppm 9.38 (s, 1H), 8.67 (t, J = 5.5 Hz, 1H), 8.18 (s, 3H), 7.79 (d, J = 7.3 Hz, 1H), 7.49 (m, 2H), 7.38 (m, 1H), 5.19 (dd, J = 7.4, 4.0 Hz, 1H), 3.68 (ddd, J = 9.9, 5.6, 4.3 Hz, 1H), 3.53 (q, J = 16.3 Hz, 1H), 3.24 (m, 1H). ^{13}C{^{1}H} NMR (100 MHz, DMSO-d_6, 298 K) δ ppm 166.1, 154.0, 132.2, 130.7, 130.7, 127.5, 121.7, 78.6, 44.4, 40.1. ESI+ MS m/z 221.11 $[M]^+$. High-resolution mass spectrometry (HRMS) (ESI) m/z $[M]^+$ calcd for $C_{10}H_{14}BN_2O_3$ 221.1092, found 221.1091.

Synthesis of ***9***. Derivative **9** was synthesized **5** following procedure A. The crude was recrystallized with hexane/EtOAc. The solid was filtered and deprotected following procedure B to give derivative **9** as an off-white solid (154.9 mg, 30%). ^{1}H NMR (400 MHz, DMSO-d_6, 298 K) δ ppm 9.30 (s, 1H), 8.85 (dt, J = 5.6 Hz, 1H), 8.52 (s, 3H), 7.90 (d, J = 8.3 Hz, 2H), 7.76 (dt, J = 7.3, 1.1 Hz, 1H). 7.58 (m, 2H), 7.45 (m, 2H), 7.36 (dt, J = 7.0, 1.10 Hz, 1H), 5.34 (dd, J = 7.7, 4.40 Hz, 1H), 4.07 (s, 2H), 3.71 (dt, J = 5.0, 13.64 Hz, 1H), 3.40 (m, 1H). ^{13}C{^{1}H} NMR (100 MHz, DMSO-d_6, 298 K) δ ppm 165.9, 154.6, 137.2, 134.2, 130.7, 130.6, 128.8, 127.4, 121.7, 78.7, 45.4, 41.8. ESI+ MS m/z 297.14 $[M]^+$. HRMS (ESI) m/z $[M]^+$ calcd for $C_{16}H_{18}BN_2O_3$ 297.1405, found 297.1402.

Synthesis of ***13***. Derivative **13** was synthesized from **5** following procedure C. The crude was purified by column chromatography on silica gel (hexane/EtOAc, 85:15) to give derivative **13** as an off-white solid (0.10 g, 24%). ^{1}H NMR (400 MHz, DMSO-d_6, 298 K) δ ppm 11.48 (s, 1 H), 9.38 (s, 1H), 8.46 (t, J = 5.2 Hz, 1H), 7.73 (dt, J = 7.3, 1.1 Hz, 1H), 7.48 (m, 2H), 7.39 (td, J = 7.1, 1.3 Hz, 1H), 5.32 (dd, J = 8.2, 3.5 Hz, 1H), 3.97 (ddd, J = 13.7, 6.1, 3.6 Hz, 1H), 3.26 (ddd, J = 13.7, 8.2, 4.5 Hz, 1H), 1.47 (s, 9H), 1.39 (s, 9H). ^{13}C{^{1}H} NMR (100 MHz, DMSO-d_6, 298 K) δ ppm 163.0, 155.5, 153.7, 152.2, 130.8, 130.7, 127.7, 121.7, 83.2, 78.4, 78.3, 45.8, 28.0, 27.6. ESI+ MS m/z 406.22 $[M + H]^+$. HRMS (ESI) m/z $[M + H]^+$ calcd for $C_{19}H_{29}BN_3O_6$ 406.2144, found 406.2164.

Synthesis of ***6***. Derivative **6** was synthesized from **13** following procedure D. The reaction mixture was concentrated under vacuum to give derivative **6** as an off-white hygroscopic solid (59.6 mg, quant.). ^{1}H NMR (400 MHz, DMSO-d_6, 298 K) δ ppm 9.43 (s, 1H), 7.78 (dt, J = 7.2, 1.0 Hz, 1H), 7.61 (t, J = 6.0 Hz, 1H), 7.52 (m, 2H), 7.39 (m, 2H), 6.96 (s), 5.23 (dd, 1 H, J = 7.7, 3.3 Hz), 3.77 (ddd, J = 14.2, 6.0, 3.4 Hz, 1H), 3.28 (ddd, J = 13.8, 7.6, 5.9 Hz, 1H). ^{13}C{^{1}H} NMR (100 MHz, DMSO-d_6, 298 K) δ ppm 157.2, 153.2, 130.8, 130.7, 127.7, 121.8, 78.6, 46.0. ESI+ MS m/z 206.11 $[M]^+$. HRMS (ESI) m/z $[M + H]^+$ calcd for $C_9H_{14}BN_3O_2$ 206.1095, found 206.1099.

Synthesis of ***14***. Derivative **14** was synthesized from **7** following procedure C. The crude was crude purified by gradient column chromatography (hexane/EtOAc, 85:15 to EtOAc/MeOH 98:2) to give derivative **14** as an off-white solid (232.0 mg, 60%). ^{1}H NMR (400 MHz, DMSO-d_6, 298 K) δ ppm 11.43 (s, 1H), 9.26 (s, 1H), 8.69 (t, J = 4.8 Hz, 1H), 8.35 (t, J = 5.6 Hz, 1H), 7.72 (dt, J = 11.4, 5.6 Hz, 1H), 7.45 (m, 2H), 7.36 (dt, J = 7.2, 1.5 Hz, 1H), 5.17 (dd, J = 7.1, 4.4 Hz, 1H), 3.93 (dd, 1 H, J = 9.6, 4.8 Hz, 2H), 3.56 (ddd, J = 13.7, 5.8, 4.5 Hz, 1H), 3.24 (ddd, J = 13.3, 7.2, 5.7 Hz, 1H), 1.48 (s, 9H), 1.38 (s, 9H). ^{13}C{^{1}H} NMR (100 MHz, DMSO-d_6, 298 K) δ ppm 167.9, 162.9, 155.0, 154.3, 151.9, 130.6, 130.5, 127.4, 121.8, 83.0, 78.7, 78.3, 44.5, 43.5, 28.0, 27.6. ESI+ MS m/z 463.24 $[M + H]^+$. HRMS (ESI) m/z $[M + H]^+$ calcd for $C_{21}H_{32}BN_4O_7$ 463.2359, found 463.2378.

Synthesis of ***8***. Derivative **8** was synthesized from **14** following procedure D. The crude was recrystallized with MeOH/Et_2O to give derivative **8** as an off-white solid (45.4 mg, 30%). ^{1}H NMR (400 MHz, DMSO-d_6, 298 K) δ ppm 9.33 (s, 1H), 8.44 (t, J = 5.6 Hz, 1H), 7.76 (dt, J = 7.2, 1.0 Hz, 1H), 7.57 (t, J = 5.9 Hz, 1H), 7.46 (m, 2H), 7.37 (td, J = 7.2, 1.4 Hz, 1H), 7.29 (s), 5.18 (dd, J = 7.6, 4.1 Hz, 1H), 3.85 (t, J = 5.6 Hz, 2H), 3.62 (ddd, J = 13.8, 5.8, 4.2 Hz, 1H), 3.20 (ddd, J = 13.8, 7.6, 5.5 Hz, 1H). ^{13}C{^{1}H} NMR (100 MHz, DMSO-d_6, 298 K) δ ppm 167.5, 157.5, 154.2, 130.7, 130.7, 127.5, 121.7, 78.8, 44.7, 43.4. ESI+ MS m/z 263.12 $[M]^+$. HRMS (ESI) m/z $[M]^+$ calcd for $C_{11}H_{16}BN_4O_3$ 263.1310, found 263.1312.

Synthesis of ***15***. Derivative **15** was synthesized from **9** following procedure C. The crude was purified by gradient column chromatography (hexane/EtOAc, 80:20 to EtOAc) to give derivative **15** as an off-white solid (139.3 mg, 55%). ^{1}H NMR (400 MHz, DMSO-d_6, 298 K) δ ppm 11.54 (s, 1H), 9.27 (s, 1H), 8.80−8.71 (m, 2H). 7.83 (m, 2H), 7.73 (dt, J = 7.3, 1.1 Hz, 1H), 7.46 (m, 2H), 7.39−3.34 (m, 3H), 5.32 (dd, J = 7.8, 4.6 Hz, 1H), 4.58 (d, J = 6.0 Hz, 2H), 3.69 (dt, J = 13.6, 5.1 Hz, 1H), 3.40 (m, 1H), 1.48 (s, 9H), 1.37 (s, 9H). ^{13}C{^{1}H} NMR (100 MHz, DMSO-d_6, 298 K) δ ppm 166.2, 163.1, 155.6, 154.5, 152.0, 141.8, 133.1, 130.7, 130.6, 127.5, 127.4, 126.9, 121.8, 83.0, 78.7, 78.4, 45.4, 43.3, 28.0, 27.7. ESI+ MS m/z 539.24 $[M + H]^+$. HRMS (ESI) m/z $[M + H]^+$ calcd for $C_{27}H_{36}BN_4O_7$ 539.2672, found 539.2697.

Synthesis of ***10***. Derivative **10** was synthesized from **15** following procedure D to give derivative **10** as an off-white solid (87.4 mg, quant.). ^{1}H NMR (400 MHz, DMSO-d_6, 298 K) δ ppm 9.28 (s, 1H), 8.80 (t, J = 5.5 Hz, 1H), 8.25 (t, J = 6.3 Hz), 7.88 (m, 2H), 7.76 (dt, J = 7.3, 1.0 Hz, 1H), 7.46 (m, 2H), 7.37 (m, 3H), 5.33 (dd, J = 7.8, 4.5 Hz, 1H), 4.46 (d, J = 6.3 Hz, 2H), 3.70 (dt, J = 13.6, 5.0 Hz, 1H), 3.39 (m, 1H). ^{13}C{^{1}H} NMR (100 MHz, DMSO-d_6, 298 K) δ ppm 166.0, 157.2, 154.6, 140.6, 133.5, 130.6, 130.6, 127.5, 127.4, 126.9, 121.7, 78.7, 45.4, 43.60. ESI+ MS m/z 339.16 $[M]^+$. HRMS (ESI) m/z $[M]^+$ calcd for $C_{17}H_{20}BN_4O_3$ 339.1623, found 339.1614.

Synthesis of ***11***. Benzylamine (0.20 g, 1.87 mmol) was guanidinylated following procedure C. The precipitate was filtered and deprotected following procedure D to give derivative **11** as a white solid (51.6 mg, 18%). ^{1}H NMR (400 MHz, DMSO-d_6, 298 K) δ ppm 8.23 (t, J = 5.9 Hz, 1H), 7.38 (m, 2H), 7.31 (m, 2H), 4.39 (d, J = 6.2 Hz, 2H). ^{13}C{^{1}H} NMR (100 MHz, DMSO-d_6, 298 K) δ ppm 157.2, 137.3, 128.5, 127.5, 127.2, 43.9. ESI+ MS m/z 150.09 $[M]^+$. HRMS (ESI) m/z $[M]^+$ calcd for $C_8H_{12}N_3$ 150.1026, found 150.1024.

Synthesis of ***4***.[37] Sialic acid (**2**) (5.00 g, 16,7 mmol) was suspended in anhydrous methanol (125 mL). TFA (1.5 mL, 19.4 mmol) was added, and the reaction was stirred at room temperature for 72 h. The solvent was evaporated under reduced pressure. The crude was triturated with Et_2O to give the sialic acid methyl ester (**4**) as a white solid (5.05, 97%). ^{1}H NMR spectra are in agreement with the literature.[37]

■ ASSOCIATED CONTENT

Supporting Information

The Supporting Information is available free of charge at https://pubs.acs.org/doi/10.1021/acs.joc.0c00173.

https://dx.doi.org/10.1021/acs.joc.0c00173
J. Org. Chem. 2020, 85, 8330−8338

NMR spectra of the receptors, ITC-binding studies, and NMR and MS spectra of the different sialic acid derivatives (**2**–**4**) with benzoboroxole, **1** (PDF)

AUTHOR INFORMATION

Corresponding Author

Paula M. Mendes − *School of Chemical Engineering, University of Birmingham, Birmingham B15 2TT, U.K.;* orcid.org/0000-0001-6937-7293; Email: p.m.mendes@bham.ac.uk

Authors

Alice Di Pasquale − *School of Chemical Engineering, University of Birmingham, Birmingham B15 2TT, U.K.*

Stefano Tommasone − *School of Chemical Engineering, University of Birmingham, Birmingham B15 2TT, U.K.;* orcid.org/0000-0001-8577-2111

Lili Xu − *School of Chemistry and Chemical Engineering, Nanjing University, Nanjing 210093, P. R. China*

Jing Ma − *School of Chemistry and Chemical Engineering, Nanjing University, Nanjing 210093, P. R. China;* orcid.org/0000-0001-5848-9775

Complete contact information is available at: https://pubs.acs.org/10.1021/acs.joc.0c00173

Author Contributions

The manuscript was written through the contributions of all authors.

Notes

The authors declare no competing financial interest.

ACKNOWLEDGMENTS

The authors acknowledge the financial support for this work from the EPSRC (EP/K027263/1), ERC (Consolidator Grant 614787), MRC (MC_PC_15032), and Prostate Cancer UK (RIA17-ST2-020). L.X. and J.M. thank Nanxin Pharm Co., Ltd., Nanjing, and Yang Ge for the technical support.

REFERENCES

(1) Traving, C.; Schauer, R. Structure, function and metabolism of sialic acids. *Cell. Mol. Life Sci.* **1998**, *54*, 1330−1349.

(2) Varki, A. Sialic acids in human health and disease. *Trends Mol. Med.* **2008**, *14*, 351−360.

(3) Schauer, R. Characterization of sialic acids. *Methods Enzymol.* **1978**, *50*, 64−89.

(4) Valianpour, F.; Abeling, N.; Duran, M.; Huijmans, J. G. M.; Kulik, W. Quantification of free sialic acid in urine by HPLC-electrospray tandem mass spectrometry: A tool for the diagnosis of sialic acid storage disease. *Clin. Chem.* **2004**, *50*, 403−409.

(5) Pearce, O. M. T.; Laubli, H. Sialic acids in cancer biology and immunity. *Glycobiology* **2016**, *26*, 111−128.

(6) Büll, C.; Stoel, M. A.; den Brok, M. H.; Adema, G. J. Sialic acids sweeten a tumor's life. *Cancer Res.* **2014**, *74*, 3199−3204.

(7) Wu, X.; Li, Z.; Chen, X. X.; Fossey, J. S.; James, T. D.; Jiang, Y. B. Selective sensing of saccharides using simple boronic acids and their aggregates. *Chem. Soc. Rev.* **2013**, *42*, 8032−8048.

(8) Berube, M.; Dowlut, M.; Hall, D. G. Benzoboroxoles as efficient glycopyranoside-binding agents in physiological conditions: Structure and selectivity of complex formation. *J. Org. Chem.* **2008**, *73*, 6471−6479.

(9) Chaudhary, P. M.; Murthy, R. V.; Yadav, R.; Kikkeri, R. A rationally designed peptidomimetic biosensor for sialic acid on cell surfaces. *Chem. Commun.* **2015**, *51*, 8112−8115.

(10) Crich, S. G.; Alberti, D.; Szabo, I.; Aime, S.; Djanashvili, K. MRI Visualization of Melanoma Cells by Targeting Overexpressed Sialic Acid with a GdIII-dota-en-pba Imaging Reporter. *Angew. Chem., Int. Ed.* **2013**, *52*, 1161−1164.

(11) Shinde, S.; El-Schich, Z.; Malakpour, A.; Wan, W.; Dizeyi, N.; Mohammadi, R.; Rurack, K.; Gjorloff Wingren, A.; Sellergren, B. Sialic Acid-Imprinted Fluorescent Core-Shell Particles for Selective Labeling of Cell Surface Glycans. *J. Am. Chem. Soc.* **2015**, *137*, 13908−13912.

(12) Wulff, G. Selective Binding to Polymers via Covalent Bonds - The Construction of Chiral Cavities as Specific Receptor-Site. *Pure Appl. Chem.* **1982**, *54*, 2093−2102.

(13) Kowalczyk, W.; Sanchez, J.; Kraaz, P.; Hutt, O. E.; Haylock, D. N.; Duggan, P. J. The binding of boronated peptides to low affinity mammalian saccharides. *Pept. Sci.* **2018**, *110*, No. e23101.

(14) Dowlut, M.; Hall, D. G. An improved class of sugar-binding boronic acids, soluble and capable of complexing glycosides in neutral water. *J. Am. Chem. Soc.* **2006**, *128*, 4226−4227.

(15) Otsuka, H.; Uchimura, E.; Koshino, H.; Okano, T.; Kataoka, K. Anomalous binding profile of phenylboronic acid with N-acetylneuraminic acid (Neu5Ac) in aqueous solution with varying pH. *J. Am. Chem. Soc.* **2003**, *125*, 3493−3502.

(16) Adamczyk-Woźniak, A.; Borys, K. M.; Sporzyński, A. Recent Developments in the Chemistry and Biological Applications of Benzoxaboroles. *Chem. Rev.* **2015**, *115*, 5224−5247.

(17) Matsumoto, A.; Stephenson-Brown, A. J.; Khan, T.; Miyazawa, T.; Cabral, H.; Kataoka, K.; Miyahara, Y. Heterocyclic boronic acids display sialic acid selective binding in a hypoxic tumor relevant acidic environment. *Chem. Sci.* **2017**, *8*, 6165−6170.

(18) Regueiro-Figueroa, M.; Djanashvili, K.; Esteban-Gomez, D.; de Blas, A.; Platas-Iglesias, C.; Rodriguez-Blas, T. Towards Selective Recognition of Sialic Acid Through Simultaneous Binding to Its cis-Diol and Carboxylate Functions. *Eur. J. Org. Chem.* **2010**, *2010*, 3237−3248.

(19) Djanashvili, K.; Frullano, L.; Peters, J. A. Molecular recognition of sialic acid end groups by phenylboronates. *Chem. − Eur. J.* **2005**, *11*, 4010−4018.

(20) Nishitani, S.; Maekawa, Y.; Sakata, T. Understanding the Molecular Structure of the Sialic Acid-Phenylboronic Acid Complex by using a Combined NMR Spectroscopy and DFT Study: Toward Sialic Acid Detection at Cell Membranes. *ChemistryOpen* **2018**, *7*, 513−519.

(21) Ueno, H.; Iwata, T.; Koshiba, N.; Takahashi, D.; Toshima, K. Design, synthesis and evaluation of a boronic acid based artificial receptor for L-DOPA in aqueous media. *Chem. Commun.* **2013**, *49*, 10403−10405.

(22) Deshayes, S.; Cabral, H.; Ishii, T.; Miura, Y.; Kobayashi, S.; Yamashita, T.; Matsumoto, A.; Miyahara, Y.; Nishiyama, N.; Kataoka, K. Phenylboronic Acid-Installed Polymeric Micelles for Targeting Sialylated Epitopes in Solid Tumors. *J. Am. Chem. Soc.* **2013**, *135*, 15501−15507.

(23) Pizer, R. Boron acid complexation reactions with polyols and alpha-hydroxy carboxylic acids: Equilibria, reaction mechanisms, saccharide recognition. *Inorg. Chim. Acta* **2017**, *467*, 194−197.

(24) Kustin, K.; Pizer, R. Temperature-Jump Study of Rate and Mechanism of Boric Acid-Tartaric Acid Complexation. *J. Am. Chem. Soc.* **1969**, *91*, 317.

(25) Mazik, M.; Cavga, H. Molecular recognition of N-acetylneuraminic acid with acyclic benzimidazolium- and amino-pyridine/guanidinium-based receptors. *J. Org. Chem.* **2007**, *72*, 831−838.

(26) Geffert, C.; Kuschel, M.; Mazik, M. Molecular Recognition of N-Acetylneuraminic Acid by Acyclic Pyridinium- and Quinolinium-Based Receptors in Aqueous Media: Recognition through Combination of Cationic and Neutral Recognition Sites. *J. Org. Chem.* **2013**, *78*, 292−300.

(27) Attrill, H.; Takazawa, H.; Witt, S.; Kelm, S.; Isecke, R.; Brossmer, R.; Ando, T.; Ishida, H.; Kiso, M.; Crocker, P. R.; van Aalten, D. M. F. The structure of siglec-7 in complex with sialosides: leads for rational structure-based inhibitor design. *Biochem. J.* **2006**, *397*, 271−278.

(28) Wright, C. S. 2.2 Å-Resolution Structure-Analysis of Two Refined N-Acetylneuraminyl-Lactose - Wheat-Germ-Agglutinin Isolectin Complexes. *J. Mol. Biol.* **1990**, *215*, 635−651.
(29) Hernandez, V. S. Benzoboroxole Derivatives for Treating Bacterial Infections. WO12/033858, 2012.
(30) Springsteen, G.; Wang, B. H. A detailed examination of boronic acid-diol complexation. *Tetrahedron* **2002**, *58*, 5291−5300.
(31) Fokkens, J.; Klebe, G. A simple protocol to estimate differences in protein binding affinity for enantiomers without prior resolution of racemates. *Angew. Chem., Int. Ed.* **2006**, *45*, 985−989.
(32) Wiskur, S. L.; Lavigne, J. L.; Metzger, A.; Tobey, S. L.; Lynch, V.; Anslyn, E. V. Thermodynamic analysis of receptors based on guanidinium/boronic acid groups for the complexation of carboxylates, alpha-hydroxycarboxylates, and diols: Driving force for binding and cooperativity. *Chem. − Eur. J.* **2004**, *10*, 3792−3804.
(33) Sun, S. G.; Fazal, M. A.; Roy, B. C.; Chandra, B.; Mallik, S. Thermodynamic studies on the recognition of flexible peptides by transition-metal complexes. *Inorg. Chem.* **2002**, *41*, 1584−1590.
(34) Dunitz, J. D. Win Some, Lose Some - Enthalpy-Entropy Compensation In Weak Intermolecular Interactions. *Chem. Biol.* **1995**, *2*, 709−712.
(35) Frisch, M. J.; Trucks, G. W.; Schlegel, H. B.; Scuseria, G. E.; Robb, M. A.; Cheeseman, J. R.; Scalmani, G.; Barone, V.; Mennucci, B.; Petersson, G. A.; Nakatsuji, H.; Caricato, M.; Li, X.; Hratchian, H. P.; Izmaylov, A. F.; Bloino, J.; Zheng, G.; Sonnenberg, J. L.; Hada, M.; Ehara, M.; Toyota, K.; Fukuda, R.; Hasegawa, J.; Ishida, M.; Nakajima, T.; Honda, Y.; Kitao, O.; Nakai, H.; Vreven, T.; Peralta, J. E., Jr.; Ogliaro, F.; Bearpark, M.; Heyd, J. J.; Brothers, E.; Kudin, K. N.; Staroverov, V. N.; Kobayashi, R.; Normand, J.; Raghavachari, K.; Rendell, A.; Burant, J. C.; Iyengar, S. S.; Tomasi, J.; Cossi, M.; Rega, N.; Millam, J. M.; Klene, M.; Knox, J. E.; Cross, J. B.; Bakken, V.; Adamo, C.; Jaramillo, J.; Gomperts, R.; Stratmann, R. E.; Yazyev, O.; Austin, A. J.; Cammi, R.; Pomelli, C.; Ochterski, J. W.; Martin, R. L.; Morokuma, K.; Zakrzewski, V. G.; Voth, G. A.; Salvador, P.; Dannenberg, J. J.; Dapprich, S.; Daniels, A. D.; Farkas; Foresman, J. B.; Ortiz, J. V.; Cioslowski, J.; Fox, D. J. *Gaussian 09*, revision D.01; Gaussian Inc: Wallingford, CT, 2013.
(36) Shapiro, A. B.; Gao, N.; Hajec, L.; McKinney, D. C. Time-dependent, reversible, oxaborole inhibition of *Escherichia coli* leucyl-tRNA synthetase measured with a continuous fluorescence assay. *Anal. Biochem.* **2012**, *431*, 48−53.
(37) Carter, T. S.; Mooibroek, T. J.; Stewart, P. F. N.; Crump, M. P.; Galan, M. C.; Davis, A. P. Platform Synthetic Lectins for Divalent Carbohydrate Recognition in Water. *Angew. Chem., Int. Ed.* **2016**, *55*, 9311−9315.

https://dx.doi.org/10.1021/acs.joc.0c00173
J. Org. Chem. 2020, 85, 8330−8338